An Embedded Compact Scheme for Biharmonic Problems in Irregular Domains

Matania Ben-Artzi, Jean-Pierre Croisille and Dalia Fishelov

Abstract In Ben-Artzi et al. (SIAM J Numer Anal 47:3087–3108 (2009), [1]) a Cartesian embedded finite difference scheme for biharmonic problems has been introduced. The design of the scheme relies on a 19-dimensional polynomial space. In this paper, we show how to simplify the implementation by introducing a directional decomposition of this space. The boundary is handled via a level-set approach. Numerical results for non convex domains demonstrate the fourth order accuracy of the scheme.

1 Introduction

Let $\Omega \subseteq \mathbb{R}^2$ be a convex domain. The problem considered here is the biharmonic problem subject to Dirichlet boundary conditions:

$$\begin{cases} \Delta^2 \psi(\mathbf{x}) = f, & \mathbf{x} \in \Omega, \\ \psi = \frac{\partial \psi}{\partial n} = 0, & \mathbf{x} \in \partial\Omega. \end{cases} \tag{1}$$

Our purpose is to calculate a high order accurate approximation to (1), by embedding Ω in a Cartesian grid. The main idea of the scheme was described in [1]. Here we extend and elaborate on the presentation in [3, Chap. 11].

M. Ben-Artzi
Institute of Mathematics, The Hebrew University, 91904 Jerusalem, Israel
e-mail: mbartzi@math.huji.ac.il

J.-P. Croisille (✉)
Department of Mathematics, IECL, UMR CNRS 7502,
Université de Lorraine, 57045 Metz, France
e-mail: jean-pierre.croisille@univ-lorraine.fr

D. Fishelov
Afeka Tel Aviv Academic College of Engineering, 218 Bnei-Efraim St.,
69107 Tel-Aviv, Israel
e-mail: daliaf@afeka.ac.il

We consider the convex domain Ω as embedded in a large uniform grid of mesh size h. A grid point is a point $Q_{i,j} = (ih, jh)$ for $i, j \in \mathbb{Z}$. Following common terminology, we use the term **interior nodes** for the grid points that lie **inside** Ω. We denote by Ω_h the ensemble of these nodes, namely:

$$\Omega_h = \left\{ Q_{i,j} \in \Omega, \quad i, j \in \mathbb{Z} \right\}. \tag{2}$$

We split the set Ω_h into two sets, $\Omega_h = \Omega_h^{calc} \cup \Omega_h^{edge}$, as follows:

- Ω_h^{calc} = the set of *calculated nodes*.
  This set consists of those nodes that are located "well within" Ω, namely sufficiently far from the boundary $\partial\Omega$. In particular, if all diagonally neighboring nodes $Q_{i\pm 1, j\pm 1}$ are in Ω_h then $Q_{i,j} \in \Omega_h^{calc}$. Remark that by convexity all eight neighboring nodes are then in Ω_h. However, it should be emphasized that even if not all its neighboring nodes are in Ω_h, a node $Q_{i,j}$ can still be considered as "calculated" if it is not "too close" to the boundary, as we explain below.
  The approximate values at the calculated nodes are obtained by the proposed scheme.
- Ω_h^{edge} = the set of *edge nodes*.
  This set consists of those nodes (interior to Ω) that are located "too close" to the boundary $\partial\Omega$. They differ from the calculated nodes in the sense that there are no approximate values associated with them. Their role is "geometric"; they serve in the determination of a set Ω_h^{bdry} of **boundary nodes** that are actually located **on the boundary** $\partial\Omega$, and carry the assigned boundary values.
- Observe that the set Ω_h^{bdry} consists of selected points on the boundary, and in general is not included in the underlying global grid $Q_{i,j}$, $i, j \in \mathbb{Z}$.

In Fig. 1 we designate the calculated nodes with black circles, whereas the edge nodes are designated by white circles.

The proposed scheme is a compact scheme, i.e. all approximate values of high order derivatives are related to values of a function ψ and its derivatives ψ_x, ψ_y at immediate neighbors. More specifically, given a node $\mathbf{M}_0 = Q_{i,j} \in \Omega_h$, we consider the eight surrounding nodes in the grid:

Fig. 1 Embedding of an elliptical domain in a Cartesian grid. Calculated nodes are represented by *black circles*. Exterior points are represented by *black squares*. The points labelled with *white circles* represent edge points, i.e. interior points close to the boundary
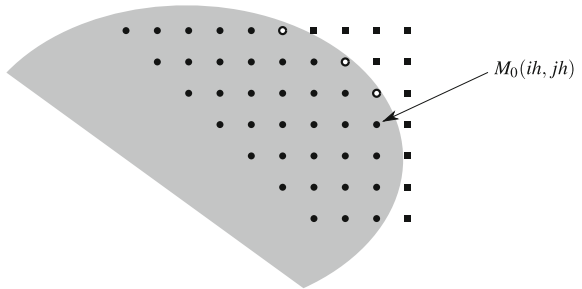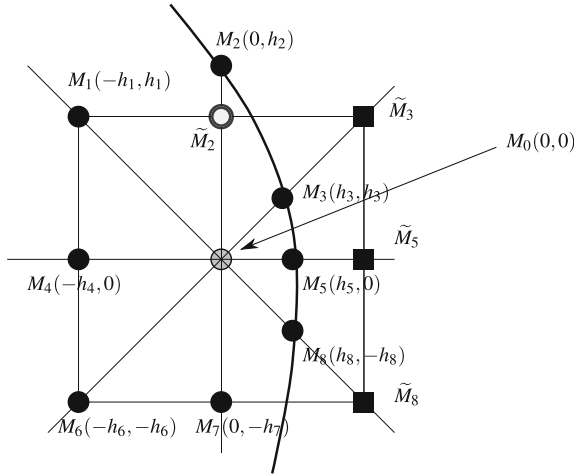
Fig. 2 Zoom on the neighborhood of point M_0 in Fig. 1. The coordinates have been moved such that M_0 is the coordinates *center*. The 8 neighbors points of M_0 are the points $\mathbf{M}_1$, $\mathbf{M}_2$, $\mathbf{M}_3$, $\mathbf{M}_4$, $\mathbf{M}_5$, $\mathbf{M}_6$, $\mathbf{M}_7$ and $\mathbf{M}_8$. The points $\mathbf{M}_1$, $\mathbf{M}_4$, $\mathbf{M}_6$ and $\mathbf{M}_7$ belong to the Cartesian grid. The points $\mathbf{M}_2$, $\mathbf{M}_3$, $\mathbf{M}_5$ and $\mathbf{M}_8$ belong to the boundary of the domain. They are obtained as the intersection of rays emanating from $\mathbf{M}_0$ and directed towards $\widetilde{\mathbf{M}}_2$, $\widetilde{\mathbf{M}}_3$, $\widetilde{\mathbf{M}}_5$ and $\widetilde{\mathbf{M}}_8$ respectively. The points $\widetilde{\mathbf{M}}_3$, $\widetilde{\mathbf{M}}_5$ and $\widetilde{\mathbf{M}}_8$ are outside the domain. The edge point above $\mathbf{M}_0$ is marked with an *open circle*

$$\widetilde{\mathbf{M}}_1 = Q_{i-1,j+1}, \quad \widetilde{\mathbf{M}}_2 = Q_{i,j+1}, \quad \widetilde{\mathbf{M}}_3 = Q_{i+1,j+1}, \widetilde{\mathbf{M}}_4 = Q_{i-1,j},$$
$$\widetilde{\mathbf{M}}_5 = Q_{i+1,j}, \quad \widetilde{\mathbf{M}}_6 = Q_{i-1,j-1}, \quad \widetilde{\mathbf{M}}_7 = Q_{i,j-1}, \widetilde{\mathbf{M}}_8 = Q_{i+1,j-1}.$$

If all the nine nodes $\widetilde{\mathbf{M}}_i$ are *calculated nodes*, namely, in Ω_h^{calc}, or coincide with a boundary point, which is part of the grid, we set $\mathbf{M}_i = \widetilde{\mathbf{M}}_i$, $i = 0, \dots, 8$, and continue with this regular stencil centered at $\mathbf{M}_0$. Otherwise, our goal is to replace the $\widetilde{\mathbf{M}}_i's$ that are not in Ω_h^{calc} by suitable $\mathbf{M}_i's$ that are boundary points, namely, in Ω_h^{bdry}. The values of ψ, ψ_x, ψ_y at these points are all that is needed in order to calculate the various approximate derivatives at $\mathbf{M}_0$.

To describe this construction, suppose that $\mathbf{M}_0 \in \Omega_h^{calc}$ is a calculated node, while for some $1 \le i \le 8$, the neighboring node $\widetilde{\mathbf{M}}_i$ is either an edge node or an exterior node. Consider the calculated node designated by $\mathbf{M_0}$ in Fig. 1. A zoom is shown on Fig. 2. The 8 points $\widetilde{\mathbf{M}}_i$ are the points in the square (4 corner points and 4 mid-edge points). Take the ray that emanates from $\mathbf{M}_0$ and goes through $\widetilde{\mathbf{M}}_i$. This ray must cross the boundary $\partial\Omega$ at exactly one point since Ω is convex. We define the intersection point as $\mathbf{M_i}$.

The calculation of the approximate value to $\Delta^2\psi(\mathbf{M_0})$ relies on the data at $\mathbf{M_i}$ rather than $\widetilde{\mathbf{M}}_i$.

- The four neighbors $\widetilde{\mathbf{M}}_1$, $\widetilde{\mathbf{M}}_4$, $\widetilde{\mathbf{M}}_6$ and $\widetilde{\mathbf{M}}_7$ are other calculated nodes so we keep them, i.e. $\widetilde{\mathbf{M}}_i = \mathbf{M}_i$, $i = 1, 4, 6, 7$. In particular, if we shift the coordinates of $\mathbf{M}_0$ to $(0, 0)$, we have for the coordinates of $\mathbf{M}_i$, $i = 1, 4, 6, 7$, the values $h_1 = h_4 = h_6 = h_7 = h$.
- The other four neighbors $\widetilde{\mathbf{M}}_2$, $\widetilde{\mathbf{M}}_3$, $\widetilde{\mathbf{M}}_5$ and $\widetilde{\mathbf{M}}_8$ are either edge or exterior nodes so they are replaced by points on the boundary as described above.

We thus obtain $\mathbf{M}_i$, the actual points used in the calculation.

Once the 8 points $\mathbf{M}_i$ are determined and approximate values ψ, ψ_x and ψ_y are assigned to them, we can proceed to evaluate an approximate value for $\Delta^2\psi$ at the point $\mathbf{M}_0$. This is described in Sect. 2.

2 The Discrete Biharmonic $\Delta_\mathbf{h}^2\psi$ Operator

In this section we present our finite-difference scheme for the approximation of the biharmonic operator. Figure 2 shows the stencil used for the approximation of $\Delta^2\psi$ at $\mathbf{M}_0 = (0, 0)$. The 8 points $\mathbf{M}_k$, $1 \le k \le 8$ form an irregular stencil around $\mathbf{M}_0$. Each of the nine grid points $\mathbf{M}_k$ carries three values: ψ, ψ_x, ψ_y. These are calculated values if $\mathbf{M}_k \in \Omega_h^{calc}$ is a calculated node. If $\mathbf{M}_k \in \Omega_h^{bdry}$, then this point carries boundary data given by the boundary conditions. In order to approximate $\Delta^2\psi$ of a given smooth function ψ at $\mathbf{M}_0$ we interpolate the data ψ, ψ_x, ψ_y on the stencil $\{\mathbf{M}_0, \ldots, \mathbf{M}_8\}$ by a certain polynomial $P_{\mathbf{M}_0}$ of degree 6. The detailed construction of $P_{\mathbf{M}_0}(x, y)$ is carried out in Sect. 3. To handle the irregular stencil around $\mathbf{M}_0$ we denote by $\mathbf{h}$ the vector of the step-sizes around $\mathbf{M}_0$, as in Fig. 2:

$$\mathbf{h} = [h_1, \ldots, h_8]^T. \tag{3}$$

Once the polynomial $P_{\mathbf{M}_0}(x, y)$ is constructed, we replace the smooth function ψ by a discrete function $\widetilde{\psi}$, defined only on the set of nodes $\Omega_h^{calc} \cup \Omega_h^{bdry}$. The discrete biharmonic operator $\Delta_\mathbf{h}^2\psi$ for the approximation of $\Delta^2\psi$ at $\mathbf{M}_0 = (0, 0)$ is then defined by

$$\Delta_\mathbf{h}^2\widetilde{\psi}(\mathbf{M}_0) = \Delta^2 P_{\mathbf{M}_0}(0, 0), \tag{4}$$

3 Calculating the Interpolation Polynomial $P_{\mathbf{M}_0}(x, y)$

As mentioned above, our compact scheme for the biharmonic problem relies on an interpolation polynomial of degree six. Such a polynomial is constructed for every calculated point $\mathbf{M}_{i,j} \in \Omega_h^{calc}$. This sixth-order polynomial is called $P_{\mathbf{M}_0}(x, y)$. It is of the form (where here and below the subscript $\mathbf{M}_0$ is omitted),

$$P(x, y) = \sum_{i=1}^{19} a_i l_i(x, y), \tag{5}$$

where the polynomials $l_i(x, y)$ are (x, y) are shifted so that $\mathbf{M}_0 = (0, 0)$:

$$
\begin{cases}
l_1(x, y) = 1, \ \ l_2(x, y) = x, \ \ l_3(x, y) = x^2, \ \ l_4(x, y) = x^3, \\
l_5(x, y) = x^4, \ \ l_6(x, y) = x^5, \ \ l_7(x, y) = y, \ \ l_8(x, y) = y^2, \ \ l_9(x, y) = y^3, \\
\qquad l_{10}(x, y) = y^4, \ \ l_{11}(x, y) = y^5, \ \ l_{12}(x, y) = xy, \\
\qquad l_{13}(x, y) = xy(x + y), \ \ l_{14}(x, y) = xy(x - y), \\
\qquad l_{15}(x, y) = xy(x + y)^2, \ \ l_{16}(x, y) = xy(x - y)^2, \\
\qquad l_{17}(x, y) = xy(x + y)^3, \ \ l_{18}(x, y) = xy(x - y)^3, \\
\qquad\qquad l_{19}(x, y) = x^2 y^2 (x^2 + y^2).
\end{cases} \tag{6}
$$

The 19 coefficients a_i are obtained as follows. We consider the discrete values depending on $\widetilde{\psi}$ located at the eight points $\mathbf{M}_k$, $1 \le k \le 8$, around the point $\mathbf{M}_0$, (see Fig. 2). From the discrete data at these points we determine 19 values to be interpolated by $P(x, y)$ and its derivatives:

$$
\begin{cases}
\Gamma_1(\psi) = \widetilde{\psi}(\mathbf{M}_1), \ \ \Gamma_2(\psi) = \widetilde{\psi}(\mathbf{M}_2), \ \ \Gamma_3(\psi) = \widetilde{\psi}(\mathbf{M}_3), \\
\Gamma_4(\psi) = \widetilde{\psi}(\mathbf{M}_4), \ \ \Gamma_5(\psi) = \widetilde{\psi}(\mathbf{M}_0), \ \ \Gamma_6(\psi) = \widetilde{\psi}(\mathbf{M}_5), \\
\Gamma_7(\psi) = \widetilde{\psi}(\mathbf{M}_6), \ \ \Gamma_8(\psi) = \widetilde{\psi}(\mathbf{M}_7), \ \ \ \Gamma_9(\psi) = \widetilde{\psi}(\mathbf{M}_8), \\[4pt]
\Gamma_{10}(\psi) = (-\partial_x + \partial_y)\widetilde{\psi}(\mathbf{M}_1), \ \ \ \Gamma_{11}(\psi) = \partial_y \widetilde{\psi}(\mathbf{M}_2), \\
\Gamma_{12}(\psi) = (\partial_x + \partial_y)\widetilde{\psi}(\mathbf{M}_3), \ \ \ \Gamma_{13}(\psi) = -\partial_x \widetilde{\psi}(\mathbf{M}_4), \\
\Gamma_{14}(\psi) = \partial_x \widetilde{\psi}(\mathbf{M}_0), \ \ \ \Gamma_{15}(\psi) = \partial_y \widetilde{\psi}(\mathbf{M}_0), \\
\Gamma_{16}(\psi) = \partial_x \widetilde{\psi}(\mathbf{M}_5), \ \ \ \Gamma_{17}(\psi) = (-\partial_x - \partial_y)\widetilde{\psi}(\mathbf{M}_6), \\
\Gamma_{18}(\psi) = -\partial_y \widetilde{\psi}(\mathbf{M}_7), \ \ \ \Gamma_{19}(\psi) = (\partial_x - \partial_y)\widetilde{\psi}(\mathbf{M}_8).
\end{cases} \tag{7}
$$

Note that the derivatives at any point are taken in the direction of $\mathbf{M}_0$ except that the full gradient is given at the point $\mathbf{M}_0$.

There is a one-to-one correspondence between the polynomial (5) and the above set of 19 data. More explicitly, the 19 coefficients a_i in (5) are uniquely determined by the data (7). For the proof of this linear algebraic fact, see [1].

In (5), the coefficients a_i depend linearly on the data $\Gamma_k(\psi), 1 \le k \le 19$. Therefore, $P(x, y)$ can be rewritten as

$$P(x, y) = \sum_{i=1}^{19} \left(\sum_{j=1}^{19} A_{i,j} \Gamma_j(\psi) \right) l_i(x, y). \tag{8}$$

We need to calculate the geometric coefficients $A_{i,j}$, $1 \leq i, j \leq 19$ in terms of the vector $\mathbf{h} = [h_1, h_2, h_3, h_4, h_5, h_6, h_7, h_8]$. For this purpose, it is useful to decompose the polynomial $P(x, y)$ into the sum of four terms

$$P(x, y) = P(0, 0) + P_1(x) + P_2(y) + xyQ(x, y). \tag{9}$$

Looking at (5) and (6), these four terms are expressed as:

$$a_1 = P(0, 0) = \psi(\mathbf{M}_0) \text{ (given value)}, \tag{10}$$

$$\begin{cases} P_1(x) = a_2 x + a_3 x^2 + a_4 x^3 + a_5 x^4 + a_6 x^5, \\ P_2(y) = a_7 y + a_8 y^2 + a_9 y^3 + a_{10} y^4 + a_{11} y^5. \end{cases} \tag{11}$$

The polynomial $Q(x, y)$ in (9) is then defined as

$$\begin{aligned} Q(x, y) &= \frac{P(x, y) - P(0, 0) - P_1(x) - P_2(y)}{xy} \\ &= a_{12} + a_{13}(x + y) + a_{14}(x - y) + a_{15}(x + y)^2 + a_{16}(x - y)^2 \qquad (12) \\ &\quad + a_{17}(x + y)^3 + a_{18}(x - y)^3 + a_{19}xy(x^2 + y^2). \qquad (13) \end{aligned}$$

This decomposition is directional in the following sense:

- The polynomial $P_1(x) \in \text{Span}\{x, x^2, x^3, x^4, x^5\}$ corresponds to the "horizontal data". It is determined by the 5 data (see Fig. 2):

$$\psi(\mathbf{M}_4), \psi(\mathbf{M}_5), \partial_x \psi(\mathbf{M}_4), \partial_x \psi(\mathbf{M}_0), \partial_x \psi(\mathbf{M}_5). \tag{14}$$

- Similarly, $P_2(y) \in \text{Span}\{y, y^2, y^3, y^4, y^5\}$ corresponds to the "vertical data". It is specified by the 5 data

$$\psi(\mathbf{M}_7), \psi(\mathbf{M}_2), \partial_y \psi(\mathbf{M}_7), \partial_y \psi(\mathbf{M}_0), \partial_y \psi(\mathbf{M}_2). \tag{15}$$

- Finally, it can be shown that the polynomial $Q(x, y)$ is determined by the 8 "diagonal data" in (7). These data are:

$$\begin{cases} \Gamma_1(\psi) = \psi(\mathbf{M}_1), \quad \Gamma_3(\psi) = \psi(\mathbf{M}_3), \quad \Gamma_7(\psi) = \psi(\mathbf{M}_6), \quad \Gamma_9(\psi) = \psi(\mathbf{M}_8), \\ \Gamma_{10}(\psi) = (-\partial_x + \partial_y)\psi(\mathbf{M}_1), \quad \Gamma_{12}(\psi) = (\partial_x + \partial y)\psi(\mathbf{M}_3), \\ \Gamma_{17}(\psi) = (-\partial_x - \partial_y)\psi(\mathbf{M}_6), \quad \Gamma_{19}(\psi) = (\partial_x - \partial_y)\psi(\mathbf{M}_8). \end{cases}$$

$$\tag{16}$$

4 The Numerical Scheme

4.1 The Embedded Discrete Biharmonic Operator

In this section, we assume given for each point of the Cartesian grid the polynomial $P(x, y)$ (5) in terms of the data $\Gamma_k(\psi)$. As explained in Sect. 3, the polynomial $P_{\mathbf{M}_0}(x, y)$ in (5) is explicitly known by the coefficients a_i, given as the analytical functions:

$$\Big[\mathbf{h}, [\Gamma_j(\psi)]\Big]_{j=1,\dots,19} \mapsto \mathbf{a} = \Big[a_1, a_2, \dots, a_{18}, a_{19}\Big]^T. \tag{17}$$

The discrete biharmonic at $\mathbf{M_0}(\mathbf{x_0}, \mathbf{y_0})$ is obtained by:

$$\Delta_{\mathbf{h}}^2 \widetilde{\psi}(\mathbf{M}_0) = \sum_{k=1}^{19} a_k \Delta^2 l_k(x_0, y_0). \tag{18}$$

There are four nonvanishing terms in the right-hand-side of (18) which are:

$$\begin{cases} \Delta^2 l_5(x_0, y_0) = 24, & \Delta^2 l_{10}(x_0, y_0) = 24, \\ \Delta^2 l_{15}(x_0, y_0) = 16, & \Delta^2 l_{16}(x_0, y_0) = -16. \end{cases} \tag{19}$$

Therefore the discrete biharmonic at $\mathbf{M}_0$ is given in terms of the coefficients $a_k\Big[\mathbf{h}, [\Gamma_j(\psi)]\Big]$ by

$$\Delta_{\mathbf{h}}^2 \psi(M_0) \triangleq 24\Big(a_5(\mathbf{h}, [\Gamma_k(\psi)]) + a_{10}(\mathbf{h}, [\Gamma_k(\psi)])\Big) \tag{20}$$

$$+ 16\Big(a_{15}(\mathbf{h}, [\Gamma_k(\psi)]) - a_{16}(\mathbf{h}, [\Gamma_k(\psi)])\Big). \tag{21}$$

The discrete equation at point $\mathbf{M}_0$ is therefore (see (4)):

$$\Delta_{\mathbf{h}}^2 \widetilde{\psi}(\mathbf{M_0}) = f(\mathbf{M_0}). \tag{22}$$

Equation (22) has to be supplemented by some additional relation connecting the derivatives $\psi_{x,i,j}$, $\psi_{y,i,j}$ and the values $\psi_{i,j}$. Our choice [1, 3] is to use an *Hermitian* relation in the x- and the y-direction. In the x-direction we have:

$$\alpha_{1,i}\psi_{x,i-1,j} + \psi_{x,i,j} + \alpha_{2,i}\psi_{x,i+1,j} = \beta_{1,i}\psi_{i-1,j} + \beta_{2,i}\psi_{i,j} + \beta_{3,i}\psi_{i+1,j}. \tag{23}$$

The five coefficients $\alpha_{1,i}$, $\alpha_{2,i}$, $\beta_{1,i}$, $\beta_{2,i}$ and $\beta_{3,i}$ are defined as follows. Let $\mathbf{M_0} = Q_{i,j}(x_i, y_j)$ and let the two neighbor points $\mathbf{M_4}$ and $\mathbf{M_5}$ be (see Fig. 2):

$$\mathbf{M_4}(x_i - h_i, y_j), \quad \mathbf{M_5}(x_i + h_{i+1}, y_j). \tag{24}$$

Then

$$\begin{cases} \alpha_{1,i} = \dfrac{h_{i+1}^2}{(h_{i+1}+h_i)^2}, & \alpha_{2,i} = \dfrac{h_i^2}{(h_{i+1}+h_i)^2}, & \beta_{2,i} = \dfrac{2h_{i+1}^4+4h_{i+1}^3 h_i - 4h_{i+1}h_i^3 - 2h_i^4}{h_{i+1}(h_{i+1}+h_i)^3 h_i}, \\[3mm] & \beta_{1,i} = -\dfrac{2h_{i+1}^4+4h_{i+1}^3 h_i}{h_{i+1}(h_{i+1}+h_i)^3 h_i}, & \beta_{3,i} = \dfrac{2h_i^4+4h_{i+1}h_i^3}{h_{i+1}(h_{i+1}+h_i)^3 h_i}. \end{cases} \tag{25}$$

In the y-direction we have

$$\gamma_{1,j}\psi_{y,i,j-1} + \psi_{y,i,j} + \gamma_{2,j}\psi_{y,i,j+1} = \delta_{1,j}\psi_{i,j-1} + \delta_{2,j}\psi_{i,j} + \delta_{3,j}\psi_{i,j+1}. \tag{26}$$

with values of the five coefficients $\gamma_{1,j}$, $\gamma_{2,j}$, $\delta_{1,j}$, $\delta_{2,j}$ and $\delta_{3,j}$ deduced from the points $\mathbf{M_7}$ and $\mathbf{M_2}$ in a way similar to (25). We refer to [1, 3] for an analysis of the Hermitian relations (23) and (26).

4.2 Assembling the Global Linear System

To each point (i,j) corresponds the discrete biharmonic relation (22) together with the horizontal and vertical Hermitian relations for the discrete gradient (23) and (26). All these relations form a linear system

$$A\Psi = F. \tag{27}$$

Assembling the matrix A using the relations (22), (23), (26) is analogous to assembling the global matrix in the finite element method.

According to Sect. 1, each point $\mathbf{M}_{i,j}$ of the Cartesian grid belongs to one of the five categories:

1. interior regular calculated point
2. interior irregular calculated point
3. interior edge point
4. boundary point
5. exterior point.

In our computation, this classification is performed using a so-called *level set* model for the boundary $\partial\Omega$. Assume that $(x,y) \mapsto \varphi(x,y)$ is a smooth function such that, at least locally

$$\varphi(x,y) \begin{cases} < 0 & \text{if } (x,y) \in \Omega, \quad \text{(interior point)}, \\ > 0 & \text{if } (x,y) \in \Omega^c, \quad \text{(exterior point)}, \\ = 0 & \text{if } (x,y) \in \partial\Omega, \quad \text{(boundary point)}. \end{cases} \tag{28}$$

Following [4], the interior point $\mathbf{M}_0 = \mathbf{M}_{i,j}$ is declared *close to* $\partial\Omega$ if $\varphi_{\min,i,j}\varphi_{\max,i,j} < 0$ where

$$\begin{cases} \varphi_{\min,i,j} = & \min(\varphi_{i-1,j}, \varphi_{i+1,j}, \varphi_{i,j+1}, \varphi_{i,j-1}, \varphi_{i,j}), \\ \varphi_{\max,i,j} = & \max(\varphi_{i-1,j}, \varphi_{i+1,j}, \varphi_{i,j+1}, \varphi_{i,j-1}, \varphi_{i,j}). \end{cases} \quad (29)$$

In this case, the following quadratic model for φ is defined around $\mathbf{M}_0$ by:

$$\varphi(\mathbf{x}) = \varphi_0 + (\nabla\varphi_0)^T.(\mathbf{x} - \mathbf{x}_0) + \frac{1}{2}(\mathbf{x} - \mathbf{x}_0)^T(D^2\varphi_0)(\mathbf{x} - \mathbf{x}_0). \quad (30)$$

In (30), $\nabla\varphi_0$ and $D^2\varphi_0$ stand for approximate values of the gradient and the Hessian of $\varphi(\mathbf{x})$ at $\mathbf{M}_0$. In the computations, centered differences for $\nabla\varphi_0$ and $D^2\varphi_0$ are used. Using the model (30) allows to determine the approximate projection $\mathbf{M}_0^*$ of the interior point $\mathbf{M}_0$ on $\partial\Omega$, [4]. This gives

$$\mathbf{M}_0 = \begin{cases} \text{calculated point} & \text{if } \text{dist}(\mathbf{M}_0, \mathbf{M}_0^*) \geq \varepsilon_{edge}, \\ \text{edge point} & \text{if } \text{dist}(\mathbf{M}_0, \mathbf{M}_0^*) < \varepsilon_{edge}. \end{cases} \quad (31)$$

where ε_{edge} is a fixed parameter. For each calculated point $\mathbf{M}_0$, the length vector $\mathbf{h} \in \mathbb{R}^8$ and the elementary matrix $A_{i,j}(\mathbf{h}) \in \mathbb{M}_{19}(\mathbb{R})$ are evaluated according to the preceding classification into regular/irregular calculated points. Finally the elements of each matrix $A_{i,j}(\mathbf{h})$ are collected in the global matrix A. In a second step, for each point $\mathbf{M}_{i,j}$, the submatrix of A corresponding to the Hermitian relations for the derivatives ψ_x and ψ_y in (23) is calculated. The global linear system $A\psi = b$ is the discrete version of the problem (1). Note that it is solved by a direct solver. Fast solvers issues in the fashion of [2, 4] will be addressed in a future work.

5 Numerical Results

We present several numerical results for the biharmonic problem with additional Laplacian term:

$$\begin{cases} \alpha\Delta^2\psi(\mathbf{x}) - \beta\Delta\psi(\mathbf{x}) = f, & \mathbf{x} \in \Omega, \\ \psi = g_1(\mathbf{x}), \quad \frac{\partial\psi}{\partial n} = g_2(\mathbf{x}), & \mathbf{x} \in \partial\Omega. \end{cases} \quad (32)$$

In each case, the domain Ω and the solution $\psi(\mathbf{x})$ are specified. The right-hand side $f(\mathbf{x})$ and the two boundary functions $g_1(\mathbf{x})$ and $g_2(\mathbf{x})$ are determined accordingly. The numerical scheme is then used to obtain an approximation for ψ based on the discrete values of f.

Table 1 Compact scheme for $\Delta^2\psi = f$. The solution is $\psi(x,y) = (1-x^2)^2(1-y^2)^2$ in the ellipse $x^2/1^2 + y^2/2^2 \leq 1$. The ellipse parameters are $(a = 1, b = 2, r = 1)$. The ellipse is embedded in the square $[-2,2] \times [-2,2]$. We present e and e_x, the l_2 errors for the stream function and for $\partial_x\psi$. The parameter for points labelled as *edge points* is $\varepsilon_{edge} = 5.10^{-3}h$

mesh	9×9	Rate	17×17	Rate	33×33	Rate	65×65
e_∞	1.1175(-2)	4.40	5.3108(-4)	3.94	3.4538(-5)	3.45	3.1596(-6)
$(e_x)_\infty$	2.3270(-2)	4.35	1.1419(-3)	3.61	9.3285(-5)	4.24	4.9262(-6)
e_2	1.7466(-2)	4.85	6.0551(-4)	4.08	3.5825(-5)	3.59	2.9702(-6)
$(e_x)_2$	3.1922(-2)	4.81	1.1402(-3)	3.79	8.2220(-5)	3.81	5.8612(-6)

Table 2 Compact scheme for $(\frac{1}{2}\Delta - \Delta^2)\psi = f$. The solution is $\psi(x,y) = 100(x^3 \ln(1+y)) + \frac{y}{1+x}$ in the ellipse $(x-0.5)^2/(0.5)^2 + (y-0.5)^2/0.3^2 \leq 1$. The ellipse parameters are $(a = 0.5, b = 0.3, r = 1)$ with center $(x_c, y_c) = (0.5, 0.5)$. The ellipse is embedded in the square $[0,1] \times [0,1]$. We present e and e_x, the l_2 errors for the stream function and for $\partial_x\psi$. The parameter for points labelled as *edge points* is $\varepsilon_{edge} = 5.10^{-3}h$

mesh	17×17	Rate	33×33	Rate	65×65	Rate	129×129
e_∞	6.9555(-6)	3.53	6.0000(-7)	4.43	2.7790(-8)	3.29	2.8334(-9)
$(e_x)_\infty$	4.0042(-4)	3.64	3.2033(-5)	4.07	1.9102(-6)	2.98	2.4215(-7)
e_2	1.1759(-6)	3.15	1.3240(-7)	4.26	6.9034(-9)	3.44	6.3715(-10)
$(e_x)_2$	7.4850(-5)	3.79	5.3933(-6)	3.98	3.4163(-7)	3.90	2.2865(-8)

5.1 Test Cases in an Ellipse

We first consider two test cases where the computational domain is an ellipse. A similar test case has already been considered in [1]. The observed accuracy is very good. The order of convergence is located approximately in the interval $I = [3, 4]$ (Tables 1 and 2).

5.2 Test Cases in Non Convex Domains

5.2.1 Star Shaped Domains

We consider first the biharmonic problem (see Example 4.3 in [4])

$$\begin{cases} \Delta^2\psi(\mathbf{x}) = 0 & \mathbf{x} \in \Omega, \\ \psi = g_1(\mathbf{x}), \quad \frac{\partial\psi}{\partial n} = g_2(\mathbf{x}), & \mathbf{x} \in \partial\Omega. \end{cases} \tag{33}$$
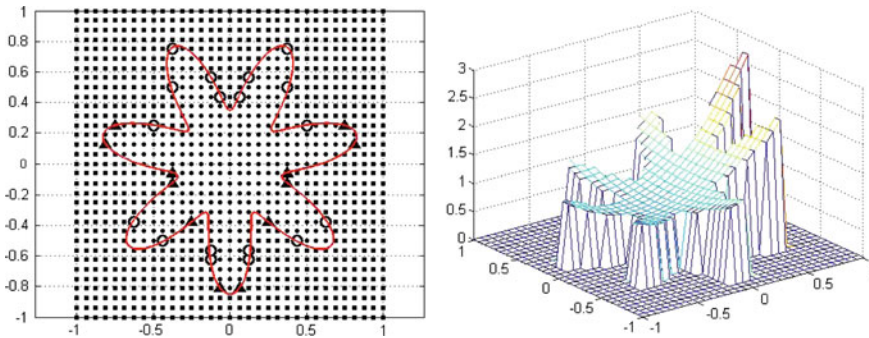
Fig. 3 Seven branches *star shaped* domain embedded in a 33×33 grid. • *Left* domain and grid. The boundary points are marked with *black triangles*. The edge points are marked with *open circles*. • *Right* approximate solution corresponding to $\psi_{ex}(x, y) = x^2 + y^2 + e^x \cos(y)$
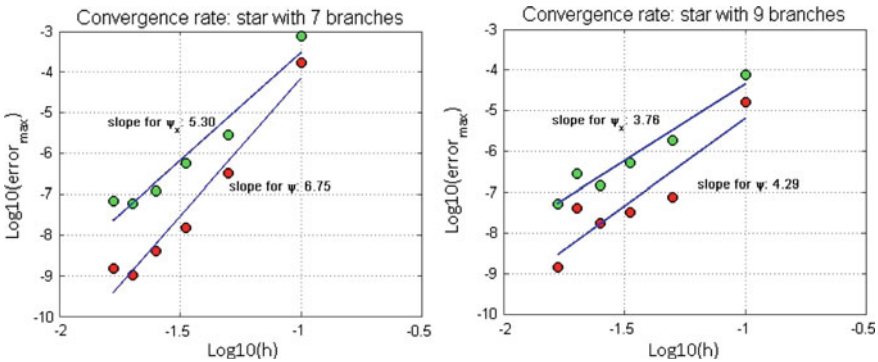

Fig. 4 Star shaped domain: linear regression of the convergence rate for $\|\Psi - \widetilde{(\psi_{ex})}\|_\infty$ and $\|\Psi_x - \widetilde{(\psi_{x,ex})}\|_\infty$ where the exact solution is $\psi_{ex}(x, y) = x^2 + y^2 + e^x \cos(y)$. • *Left* domain with 7 branches, $(k_p = 7)$. • *Right* domain with 9 branches, $(k_p = 9)$. On each regression line, the six points correspond to the six grids 10×10, 20×20, 30×30, 40×40, 50×50 and 60×60

The boundary of the domain is given in polar coordinates by

$$x(\theta) = R(\theta) \cos(\theta), \quad y(\theta) = R(\theta) \sin(\theta), \quad 0 \le \theta < 2\pi, \tag{34}$$

with $R(\theta) = 0.6 + 0.25 \sin(k_p \theta)$. The domain is represented in Fig. 3 for $k_p = 7$, (seven branches case). The exact solution is $\psi(x, y) = x^2 + y^2 + e^x \cos(y)$. The numerical results are reported in Fig. 4 where the least square slope is represented, based on six grids. They show excellent accuracy, even for very coarse grids. Observe in addition the low error level for ψ and $\partial_x \psi$.

5.2.2   A Double Circle Shaped Domain

Finally we consider the domain which consists of the interior of two disks partially overlapping. The boundary is given in polar coordinates by

$$x(\theta) = R(\theta)\cos(\theta), \quad y(\theta) = R(\theta)\sin(\theta), \quad 0 \le \theta < 2\pi. \tag{35}$$

with $R(\theta) = d|\cos(\theta)| + \sqrt{R^2 - d^2\sin(\theta)^2}$. We consider the case $R = 0.5$ and $d = 0.4$. The domain is represented in Fig. 5. The exact solution is $\psi(x, y) = \exp(x + y)$. The numerical results are reported in Fig. 6. Again, the accuracy is very good. But the levels of error are higher than in the flower case. This can be attributed to the non regular boundary.
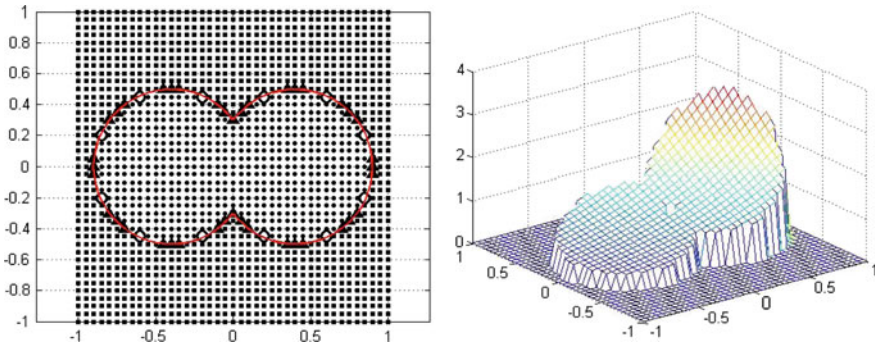

Fig. 5 Double circle shaped domain embedded in a 41×41 grid. *Left* domain and grid. The boundary points are marked with *black triangles*. The edge points are marked with *open cicles*. *Right* approximate solution $\psi(x, y) = \exp(x + y)$
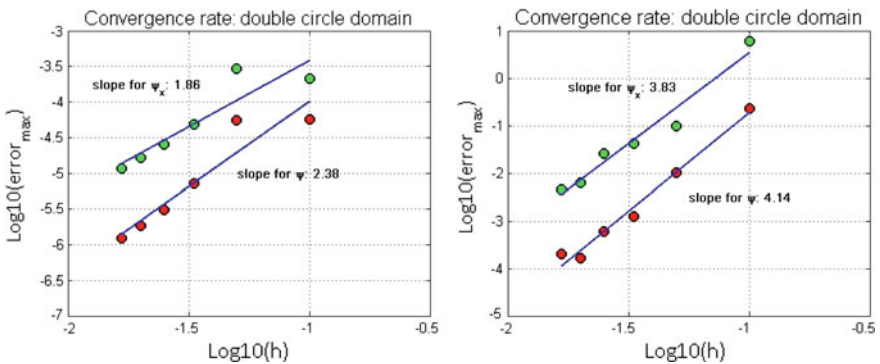

Fig. 6 Double circle shaped domain: linear regression and convergence rate for $\|\Psi - \widetilde{(\psi_{ex})}\|_\infty$ and $\|\Psi_x - \widetilde{(\psi_{x,ex})}\|_\infty$ with • *Left* $\psi_{ex}(x, y) = \exp(x + y)$ • *Right* $\psi_{ex}(x, y) = 10(x^5\sin(4\pi y) + \frac{y^4}{1+x^2})$. For each regression line, the six points correspond to the six grids 10×10, 20×20, 30×30, 40×40, 50×50 and 60×60

References

1. Ben-Artzi, M., Chorev, I., Croisille, J.-P., Fishelov, D.: A compact difference scheme for the biharmonic equation in planar irregular domains. SIAM J. Numer. Anal. **47**, 3087–3108 (2009)
2. Ben-Artzi, M., Croisille, J.-P., Fishelov, D.: A fast direct solver for the biharmonic problem in a rectangular grid. SIAM J. Sci. Comput. **31**, 303–333 (2008)
3. Ben-Artzi M., Croisille J.-P., Fishelov, D.: Navier-Stokes Equations in Planar Domains. Imperial College Press (2013)
4. Chen, G., Li, Z., Lin, P.: A fast finite difference method for biharmonic equations on irregular domains and its application to an incompressible Stokes flow. Adv. Comput. Math. **2008**, 113–133 (2008)